# Ab initio simulations of non-stoichiometric lithium—oxygen clusters

## Fabio Finocchi, Tristan Albaret and Claudine Noguera\*

Laboratoire de Physique des Solides (URA 2), Bât. 510, Université Paris-Sud, 91405 Orsay, France

Bonding and electronic properties of non-stoichiometric lithium oxide clusters  $\text{Li}_n O_2$  ( $n \leq 10$ ) are studied by means of *ab initio* simulations. We focus on the first stage of lithium enrichment of stoichiometric  $\text{Li}_4 O_2$ , where the formation of additional Li—O bonds is favoured. The bonding configuration of the lowest-energy isomers and their stability are analysed in detail, and their structures compared to those found in bulk non-stoichiometric alkali-metal suboxides. As a function of the increasing number of excess Li atoms, coexistence of an ionic and a delocalized character of the electronic density takes place, accompanied by a progressive Li—O bond weakening. These issues, and the existence of odd—even staggering of electronic properties, are discussed, in relation to recent experiments and other anion-deficient systems such as defective oxide surfaces and alkali-metal halide clusters.

#### 1 Introduction

Non-stoichiometry in oxide materials is known to change drastically their intrinsic properties and give rise to a variety of optical, catalytic and electrical conductivity phenomena which are absent in the pure material. On most oxide surfaces, the predominant type of defects formed when samples are heated or exposed to particle beams consist of oxygen vacancies. It has been shown that their presence may induce surface reconstructions, with surface cell sizes which depend upon the annealing temperature, *i.e.* upon the vacancy density. They are also responsible for enhanced reactivity, for example in water dissociation or other catalytic reactions.

The understanding of oxide clusters is by far less advanced than their bulk or surface counterparts, whether they are stoichiometric or non-stoichiometric. However, owing to their importance in chemistry and physics, it is essential to understand the variations in their physico-chemical properties as a function of their size. Unsupported, mass-selected Mg, Ca and Ba oxide,  $^{3-6}$  caesium oxide,  $^{7-9}$  and lithium oxide clusters  $^{10,11}$  have only recently been obtained and studied. In particular, a thorough study of small mass-selected oxidized lithium clusters  $^{10,11}$  has evidenced interesting systematic trends in the relative abundance of  $\text{Li}_n O_m$  species as a function of n ( $0 \le n \le 10$ ) at constant number m of oxygen atoms ( $0 \le m \le 6$ ). It has been shown that the odd–even oscillations which are generally seen in abundance spectra and ionization potentials in metallic clusters, progressively weaken and vanish when the oxygen content increases. On more general grounds, the question of whether electronic or geometric effects drive the odd–even oscillations has been raised, together with the question of the degree of localization of the excess electrons in these clusters.

From a theoretical viewpoint, several studies of stoichiometric oxide clusters have been performed, either using simple ionic models and a global optimization strategy able to find the many local minima, <sup>12</sup> or using *ab initio*, <sup>13–15</sup> or semi-empirical Hartree–Fock <sup>16</sup> approaches without a search for global minima. Focusing on stoichiometric Li<sub>2</sub>O small clusters, we have shown <sup>17</sup> that *ab initio* molecular dynamics (AIMD) simulations <sup>18</sup> are an effective tool for the investigation of such systems, in which the mixed iono–covalent character of the metal–oxygen bond and the details of the charge distributions are sensitive functions of the actual coordination of the atoms. In non-stoichiometric clusters, the need for an accurate description of the ground state is even more crucial, since the removal of oxygen atoms is expected to induce important charge redistributions as well as structural modifications, as it does in the bulk and on the surfaces of metal oxides. The possibility of strong electron redistributions raises doubts on the usefulness of empirical ionic models, whose parameters, and especially the charge values, will no longer be transferable between systems of different stoichiometry.

In this work, we report the results of AIMD simulations for small  $\operatorname{Li}_{4+p}O_2$  clusters. Starting from the stoichiometric  $\operatorname{Li}_4O_2$  parents, we consider the progressive growth of the cluster by enrichment of lithiums, in its first stages (p ranging from 0 to 6). We will only discuss the properties of clusters in which all the lithium atoms are bound to oxygens and discard isomers in which bonding to other lithiums occur. The thorough investigation of the first stages of adsorption permits us to analyse trends in the evolution of the cluster morphology and electronic structure and is a necessary premise to understanding the large-p regime.

The paper is organized as follows: we briefly describe the computational method used in the simulations, in Section 2. The results for the morphology and the bond characteristics of the lowest energy isomers are presented in Section 3. In Sections 4 and 5 trends in the evolution of the electronic structure and attachment energy of lithiums on  $\text{Li}_{4+p}\text{O}_2$  are discussed as a function of the excess number, p, of Li atoms. Section 6 ends the paper with a comparison between the oxygen-deficient lithium oxide clusters and other non-stoichiometric systems. It also contains a critical discussion of the theoretical approaches designed for these systems.

# 2 Computational details

The electronic structure calculations have been performed within the density functional theory, by using both local density approximation (LDA) and local spin density approximation (LSDA) for the exchange and correlation energy. In particular, LSDA is used for clusters with an odd number of electrons, and for some even-numbered clusters that could present a non-spin-paired ground state. We have thus checked the stability of the calculated electronic structure with respect to spontaneous spin polarization.

The Kohn-Sham orbitals are expanded in a plane-wave basis set, and soft, norm-conserving pseudopotentials are used to describe the interaction between the ionic cores (1s atomic states both for Li and oxygen), and the valence electrons. The choice of the supercell is the same as in our previous study of stoichiometric lithium oxide clusters. The pseudopotentials are used in the Kleinman-Bylander representation including s, p and d components for oxygen, and s and p components for Li. A local reference potential is chosen (d-component for O, s-component for Li). In order to obtain an optimal total energy convergence as a function of the size of the basis set, as determined by the cut-off kinetic energy,  $E_{\rm cut}$ , we followed the prescriptions given by Troullier and Martins in the generation of the O pseudopotential. The core radii chosen for O are 1.38 a.u., 1.75 a.u. and 1.38 a.u. for the s, p and d components, respectively. For this pseudopotential, the total energy of the Li<sub>2</sub>O molecule is converged within 0.5 and 0.1 eV at 39 and 60 Ry cut-off, respectively. Since the Li pseudopotential converges faster than that of oxygen as a function of  $E_{\rm cut}$ , we choose rather small cut-off radii, equal to 1.75 a.u. for both s and p components, in order to have better transferability, from the stoichiometric Li<sub>2</sub>O molecule and bulk Li<sub>2</sub>O, to pure metallic Li<sub>n</sub> clusters.

The pseudopotentials have already been tested in the study of stoichiometric lithium oxide clusters. Further test calculations have been performed on pure Li systems. For the Li dimer, excellent agreement is found with experiments and other calculations.<sup>21</sup> The calculated equilibrium distance is equal to 2.69 Å and the dissociation energy to 1.02 eV. For Li<sub>5</sub> clusters, the planar  $C_{2v}$  structure turned out to be less stable than the double-tetrahedra configuration by 0.25 eV, at variance with a previous Hartree–Fock calculation,<sup>22</sup> which predicted that the planar isomer is 0.34 eV lower in energy. However, the a posteriori inclusion of correlations reduces the energy difference to 0.17 eV. The importance of a self-consistent and accurate description of correlation effects in Li<sub>n</sub> clusters had already been pointed out.<sup>23</sup> In the case of Li<sub>6</sub>, it was shown that the stability of the three isomers, of point symmetry  $C_{2v}$ ,  $C_{5v}$  and  $D_{3h}$  can be completely reversed, depending upon the treatment of correlation effects. Fully self-consistent calculations of exchange and correlation energy in the generalized-gradient approximation unambiguously give the  $C_{2v}$ - $C_{5v}$ - $D_{3h}$  sequence, from the most to the least stable isomer. The ordering agrees with our LDA results, apart from the fact that the precise values of the energy differences that we found between the isomers are overestimated by ca. 0.1 eV. This quantitative discrepancy is attributed to the use of LDA, but it is found to have little influence on our results on  $Li_nO_2$  clusters.

In order to find out the equilibrium geometries of  $\operatorname{Li}_{4+p}O_2$  clusters, we performed some simulated annealing runs. Moreover, from the geometries resulting from the dynamic runs, we obtain other starting configurations by changing manually the local topology of the clusters. The resulting geometries are then optimized until the atomic forces do not exceed 0.005 eV Å<sup>-1</sup>, and the calculated electronic structures thus refer to the stable configuration optimized in a fully self-consistent way. The stability of all the configurations issued from the local minimizations has been checked against a random displacement of the atomic coordinates.

## 3 Morphology

We have focused on  $\operatorname{Li}_{4+p} O_2$  clusters  $(0 \le p \le 6)$ , containing two oxygen atoms and an increasing number of attached lithiums, starting from the stoichiometric compounds  $\operatorname{Li}_4 O_2$ . In a previous study,<sup>17</sup> we showed that the two most stable  $\operatorname{Li}_4 O_2$  isomers have  $D_{2h}$  and  $C_{3v}$  symmetries, as shown in Fig. 1. The  $D_{2h}$ - $\operatorname{Li}_4 O_2$  isomer has a planar structure with the oxygen atoms connected by two bridging lithiums, denoted  $\operatorname{Li}^{(2)}$ . The two remaining lithiums are singly coordinated and will be denoted  $\operatorname{Li}^{(1)}$ . The central part of the cluster presents a rhombohedral  $\operatorname{Li}_2 O_2$  ring as in the bulk antifluorite structure. By contrast, the  $C_{3v}$ - $\operatorname{Li}_4 O_2$  isomer is not planar and contains three  $\operatorname{Li}^{(2)}$  atoms and one  $\operatorname{Li}^{(1)}$ . Those two isomers are very close in energy.

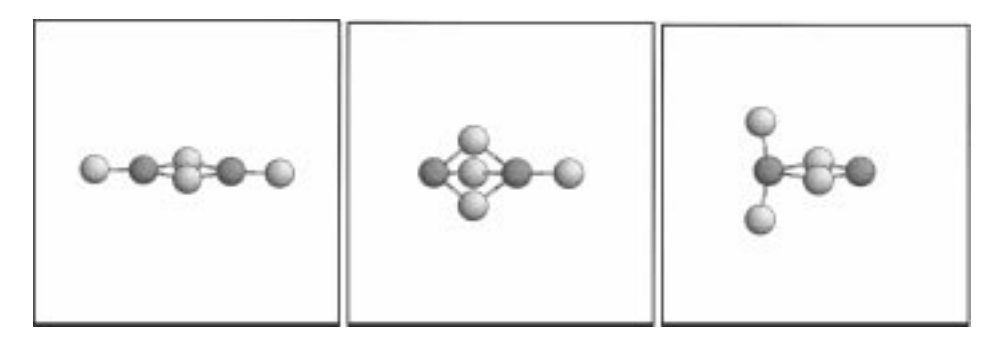


Fig. 1  $D_{2h}$ ,  $C_{3v}$  and  $C_{2v}$ -Li<sub>4</sub>O<sub>2</sub> isomers (from left to right). Li atoms are drawn in light grey, O atoms in dark grey, in all ball and stick representations. Only Li—O bonds are drawn.

The small energy difference between the  $D_{2h}$  and  $C_{3v}$  isomers results from a partial cancellation between nearest-neighbour attractive Li–O and repulsive Li–Li interactions (6 Li–O and 1 Li–Li shortest bonds in  $D_{2h}$ -Li $_4$ O $_2$ , compared with 7 Li–O and 3 Li–Li bonds in  $C_{3v}$ -Li $_4$ O $_2$ ). It can be accounted for, by using a simple pairwise potential of the type:

$$V_{ij}(r) = \frac{q_i \, q_j}{r} + A_{ij} \, \exp \left( -\beta_{ij} r \right) \tag{3.1}$$

whose parameters are adjusted to reproduce the stretching frequencies  $v_{\rm as}$  and  $v_{\rm ss}$  of the Li<sub>2</sub>O molecule, and the lattice parameter  $a_0$  and the bulk modulus  $B_0$  of the antifluorite Li<sub>2</sub>O.<sup>17</sup> This atomistic approach, although very rough, correctly accounts for the relative stability of the two isomers and gives a good estimate of their 0.16 eV energy difference. A similar ionic approach, applied to Cs<sub>4</sub>O<sub>2</sub> clusters,<sup>24</sup> predicted the same topology for the two lowest-energy isomers. Interestingly, the energy ordering of the  $C_{3v}$  and  $D_{2h}$  isomers was reversed, an indication of the delicate balance between attractive and repulsive Coulomb interactions. The pair model also predicts that the competing structure  $C_{2v}$ -Li<sub>4</sub>O<sub>2</sub> (see Fig. 1), which has 6 Li—O and 2 Li—Li short bonds, is much higher in energy, as confirmed by *ab initio* calculations.

As a result of the AIMD simulations, we found that the structures of nonstoichiometric isomers are related to those of the two most stable Li<sub>4</sub>O<sub>2</sub> parents, with attachment of additional lithiums on the oxygens, without topological change of the central part of the cluster. We will thus denote, by II-Li<sub>n</sub>O<sub>2</sub>, the isomers in which the two oxygens are bridged by two  $\operatorname{Li}^{(2)}$ , as in  $D_{2h}$ - $\operatorname{Li}_4O_2$ , and, by III- $\operatorname{Li}_nO_2$ , those in which the two oxygens are bridged by three  $\operatorname{Li}^{(2)}$ , as in  $C_{3v}$ - $\operatorname{Li}_4O_2$ . The former contain (n-2) one-fold coordinated  $\operatorname{Li}^{(1)}$  lithiums and the latter (n-3), as shown in Fig. 2. Other geometries, such as isomers with a single Li<sup>(2)</sup>, or configurations built from a pure lithium cluster with the two oxygens outside, are much higher in energy or spontaneously rearrange to more stable isomers. However, a second mechanism of growth exists, yielding clusters in which some lithiums are bound to other lithium atoms, rather than to oxygens. Such a process will undoubtedly dominate the growth to the limit of a very large number of excess lithiums. We find that the crossover between the two regimes occurs at n = 8. Up to n = 7, the most stable isomers have all their lithiums bound to oxygens. Beyond this size, metastable II-Li<sub>n</sub>O<sub>2</sub> ( $n \le 10$ ) and III-Li<sub>n</sub>O<sub>2</sub> ( $n \le 9$ ) clusters are, nevertheless, found, at energies only slightly larger than the most stable isomers. As already said in the Introduction, we will focus here on the clusters which contain only Li<sup>(1)</sup> and Li<sup>(2)</sup> lithiums and which are shown in Fig. 2. It is of interest to understand how their properties evolve as a function of their size over the whole range of *n* values where they present a (meta)stable structure.

# 3.1 II-Li<sub>n</sub>O<sub>2</sub> isomers

In the family derived from  $D_{2h}$ -Li<sub>4</sub>O<sub>2</sub>, the Li<sub>n</sub>O<sub>2</sub> clusters with n even have a mirror symmetry plane, perpendicular to the oxygen-oxygen axis and containing the two Li<sup>(2)</sup> atoms. When n is odd, this symmetry operation does not exist, since the two oxygens have inequivalent local environments.

 $\text{Li}_5 O_2$  has a  $C_{2v}$  point group symmetry. The oxygens are bound to one and two  $\text{Li}^{(1)}$  atoms, respectively. The two  $\text{Li}^{(1)}$  which are located on the same side of the cluster form a triangle with their first-neighbour oxygen, in a plane perpendicular to the rest of the cluster. Their distance to the two  $\text{Li}^{(2)}$  atoms is of the same order of magnitude as in bulk Li (3.05 cf. 3.023 Å).

In  $\text{Li}_6\text{O}_2$ , the point group symmetry is  $C_{2\text{v}}$ . The four  $\text{Li}^{(1)}$  atoms are located in a plane perpendicular to the central  $\text{Li}_2\text{O}_2$  rhombus. In addition, a large displacement of

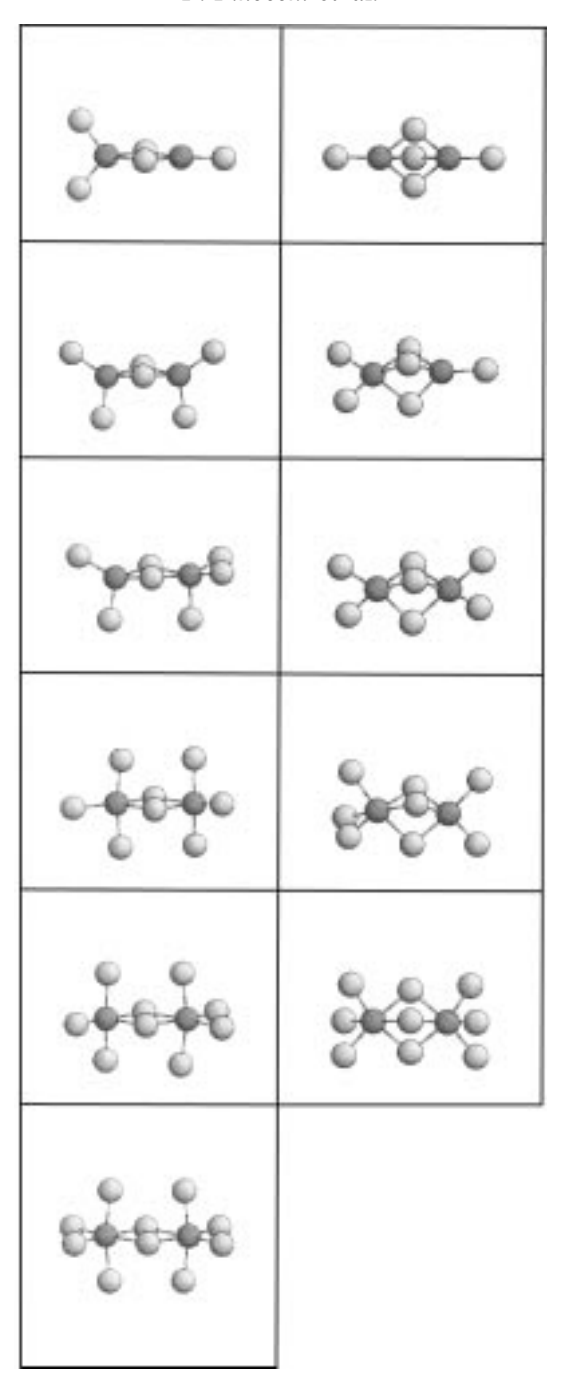


Fig. 2  $\text{Li}_{4+p} O_2$  most stable isomers, obtained by attachment of lithiums on oxygens ( $1 \le p \le 6$ ). The clusters drawn in the left and right columns belong to the II- and III-families, respectively. Li atoms are drawn in light grey, O atoms in dark grey, in all ball and stick representations. Only Li—O bonds are drawn.

two Li<sup>(1)</sup> located on opposite sides of the cluster (see Fig. 2) is found, suggesting the formation of an Li—Li bond. To confirm that this is the most stable structure, we performed a few simulations starting from initial configurations in which the four Li<sup>(1)</sup> are equivalent by symmetry. In all cases, a spontaneous atomic rearrangement took place, leading to the  $C_{2v}$  structure. This spontaneous distortion is similar to a Jahn–Teller effect and leads to the largest energy stabilization (see Section 4.2).

 ${\rm Li_7O_2}$  has a configuration very close to  ${\rm Li_6O_2}$ , with an additional  ${\rm Li^{(1)}}$  bound to one oxygen. This latter becomes five-fold coordinated and its local environment is a truncated octahedron. The overall point group symmetry of the cluster is  $C_s$ .

cated octahedron. The overall point group symmetry of the cluster is  $C_s$ . In  $\text{Li}_8\text{O}_2$ , two Li—Li bonds are formed between two pairs of  $\text{Li}^{(1)}$  atoms belonging to opposite ends of the cluster, probably to lower the total energy as the  $\text{Li}_6\text{O}_2$  (see Section 4.2). As in the latter cluster, the point group symmetry is  $C_{2v}$ .

In  $\text{Li}_9 \text{O}_2$  and  $\text{Li}_{10} \text{O}_2$ , an octahedral environment of lithium is progressively completed around the oxygens. The point group symmetries of the clusters are  $C_s$  and  $D_{2h}$ , respectively.  $\text{Li}_{10} \text{O}_2$  can be viewed as resulting from the association of two  $\text{Li}_6 \text{O}$  octahedra sharing an edge made of two  $\text{Li}^{(2)}$  atoms. Formation of six Li—O bonds around each oxygen marks the final step of stable lithium attachment that we found. We will see in Section 3.2 that the same is true for III- $\text{Li}_n \text{O}_2$  isomers.

# 3.2 III-Li<sub>n</sub>O<sub>2</sub> isomers

In the family derived from  $C_{3v}$ -Li<sub>4</sub>O<sub>2</sub>, the central Li<sub>3</sub>O<sub>2</sub> unit has a three-fold symmetry axis. In addition, a symmetry plane exists for odd values of n, at variance with II-Li<sub>n</sub>O<sub>2</sub> isomers. This plane is perpendicular to the oxygen–oxygen axis and contains the three Li<sup>(2)</sup> atoms. When n is even, the local environments of the two oxygens are inequivalent.

In  $\text{Li}_5\text{O}_2$ , the two oxygens and the two  $\text{Li}^{(1)}$  atoms are aligned along a normal to the  $\text{Li}^{(2)}$  plane, which results in a  $C_{3h}$  point group symmetry.

 $Li_6O_2$  and  $Li_7O_2$  clusters have a  $C_s$  symmetry and display an increasing number of short  $Li^{(1)}$ — $Li^{(2)}$  interatomic distances, of ca. 2.6 Å as in the  $Li_2$  dimer (2.69 Å). This suggests that  $Li^{(1)}$ — $Li^{(2)}$  bonds are formed.

In  $\text{Li}_8\text{O}_2$  and  $\text{Li}_9\text{O}_2$  clusters, progressive completion of an octahedral environment for the oxygens is achieved. The point group symmetries of the clusters are  $C_{\rm s}$  and  $C_{\rm 2v}$ , respectively. However, in  $\text{Li}_9\text{O}_2$ , the distortion which prevents the invariance by rotation of  $2\pi/3$  around the oxygen-oxygen axis is very small (ca. 0.5%).  $\text{Li}_9\text{O}_2$  results from the association of two  $\text{Li}_6\text{O}$  octahedra sharing a face. No (meta)stable isomer of this family could be found by attachment of additional lithiums.

#### 3.3 Analogy with alkali-metal suboxides

Simulation thus provides complementary information to experiment, especially as regards the equilibrium geometry of the clusters, which cannot be directly observed. Since many metastable isomers exist, the reliability of our results has to be assessed. A good confirmation comes from a study of bulk alkali-metal suboxides performed two decades ago. Crystalline suboxides of caesium and rubidium, such as  $Rb_6O$ ,  $Rb_9O_2$ ,  $Cs_7O$ ,  $Cs_4O$  and  $Cs_{11}O_3$ , were synthesized. Their structures were discussed in terms of discrete clusters of composition  $Rb_9O_2$  and  $Cs_{11}O_3$ , intercalated with purely metallic regions in the more metal-rich compounds (e.g.  $Rb_6O = [Rb_9O_2]Rb_3$ ). The  $Rb_9O_2$  clusters are two face-sharing coordination octahedra, each consisting of an oxygen atom surrounded by six Rb atoms. They are isostructural with the III-Li<sub>9</sub>O<sub>2</sub> clusters that we have obtained in our simulation. The  $Cs_{11}O_3$  units were recognized as also built from two face-sharing coordination octahedra upon which is added a third octahedron, which shares adjacent faces with the others. These are the only units serving as building blocks in the crystalline suboxides. Further addition of metal atoms results in a phase separa-

tion rather than addition to the unit itself. Our findings support this conclusion. First, we were not able to find stable (or metastable) clusters in which the oxygen coordination number was larger than six. Moreover, the stability of the local octahedral environment for the oxygens is reflected in the fact that the simulation produced the III-Li<sub>9</sub>O<sub>2</sub> cluster, the II-Li<sub>10</sub>O<sub>2</sub> cluster and an Li<sub>11</sub>O<sub>2</sub> isomer, in which six-fold coordinated oxygens are bridged by three, two and one Li<sup>(2)</sup>, respectively. These represent the three possible ways to connect two octahedra (by a face, an edge or a vertex). It can be hypothesized that the eight-fold coordination found in the antifluorite structure is not stable as a local environment of an isolated oxygen, but requires a larger ratio of oxygen to metal atoms.

## 3.4 Analysis of interatomic distances

According to the first models by Born and Madelung, ionic solids are described as a pile of positively and negatively charged spheres, held together by attractive Coulomb interactions between anions and cations. These models were sustained by the observation that an approximately constant radius, the so-called ionic radius, could be assigned to each ion, the anion–cation shortest interatomic distance being in most cases equal to the sum of ionic radii. Later, it was recognized that small variations in the ionic radii have to be introduced when the local environment of the ions changes. As a qualitative trend, the larger the coordination number, the larger the ionic radius. In our previous study of stoichiometric  $\operatorname{Li}_{2n}O_n$  clusters, we analysed the oxygen–lithium first-neighbour distances, over a wide range of different local environments. We pointed out that the mean bond lengths  $\bar{d}(O^{(p)})$  and  $\bar{d}(\operatorname{Li}^{(p)})$  around a p-fold coordinated oxygen or lithium, respectively, are increasing functions of p. The two families of non-stoichiometric  $\operatorname{Li}_{4+p}O_2$  clusters also display a wide variety of  $\operatorname{Li}$ —O bonds, owing to the increasing coordination of the oxygens in each family. In addition, extra bond distortion could be induced by the non-stoichiometry.

Fig. 3 shows the variations in the first-neighbour Li-O distances (in Å) as a function of both the lithium and the oxygen coordination numbers. As in the stoichiometric clusters, the Li<sup>(1)</sup>-O bond lengths are systematically shorter than their Li<sup>(2)</sup>-O counterparts for a given p value, *i.e.* for a given oxygen environment. Moreover, a large bond stretching takes place when the coordination of the oxygen increases, for both Li<sup>(1)</sup> and Li<sup>(2)</sup> atoms. The effect is ca. 12–13% when one compares Li-O<sup>(3)</sup> and Li-O<sup>(6)</sup> bonds. Part of the dilatation effect may be assigned to the Li-Li repulsion which increases as a function of the oxygen coordination number.

However, quantitatively, the slope of the Li—O distances vs. p curves is much larger than in the stoichiometric clusters. In the latter, the maximum expansion of Li<sup>(1)</sup>—O and Li<sup>(2)</sup>—O bonds only amounts to 2% and 6%, respectively. In the non-stoichiometric clusters, the Li—O bond lengths are, thus, not only fixed by the local environment of the atoms but also by the overall electronic structure of the cluster. Starting from the Li<sub>4</sub>O<sub>2</sub> parent, the addition of each neutral lithium brings one excess electron, which is redistributed in the cluster, thus changing the ionic charges. It may be anticipated from observation of Li—O bond stretching that the excess electrons are (at least partially) borne by the lithiums, thus reducing their attractive interaction with the oxygens. The following section is devoted to a more thorough investigation of this effect.

We conclude this section by some additional remarks on the geometry of the III-Li<sub>9</sub>O<sub>2</sub> isomer. As mentioned above, this isomer is isostructural with the Rb<sub>9</sub>O<sub>2</sub> cluster which serves as a building block in crystalline Rb<sub>9</sub>O<sub>2</sub> and Rb<sub>6</sub>O suboxides. It was noted by the author of ref. 25 that the characteristic distances in Rb<sub>9</sub>O<sub>2</sub> clusters are close to those observed in bulk Rb<sub>2</sub>O, and that the oxygens are shifted from the octahedron centre towards the outer Rb atoms, so as to increase the O—O distance. Both conclusions hold in III-Li<sub>9</sub>O<sub>2</sub>. The shift of the oxygens is due to the inequivalence of Li<sup>(1)</sup> and

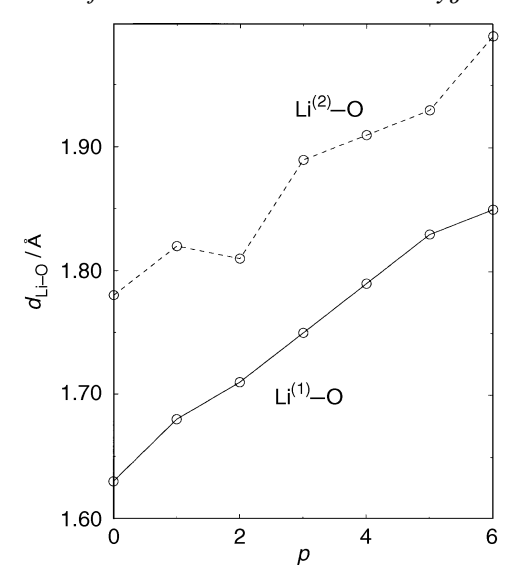


Fig. 3 Lithium-oxygen interatomic distances in the symmetric  $\text{Li}_{4+p}\text{O}_2$  clusters (II-isomers when p is even and family III-isomers when p is odd). Full and dashed lines refer to  $\text{Li}^{(1)}$ —O and  $\text{Li}^{(2)}$ —O bond lengths, respectively.

Li<sup>(2)</sup>, the Li<sup>(2)</sup>—O bonds being longer than the Li<sup>(1)</sup>—O bonds. The mean Li—O interatomic distances in III-Li<sub>9</sub>O<sub>2</sub> (1.99 Å) are also close to those observed in bulk Li<sub>2</sub>O (1.97 Å). This is the result of the competition between bond contraction associated with the decrease in coordination (O<sup>(6)</sup>, Li<sup>(1)</sup> and Li<sup>(2)</sup> in III-Li<sub>9</sub>O<sub>2</sub>, cf. O<sup>(8)</sup> and Li<sup>(4)</sup> in bulk Li<sub>2</sub>O) and bond expansion induced by the non-stoichiometry in the cluster.

# 4 Electronic structure

Bulk  $\text{Li}_2\text{O}$  is a very ionic insulating oxide whose electronic structure displays a valence band, mainly built from oxygen orbitals, and a conduction band of mainly lithium character. These features are shared by the stoichiometric  $\text{Li}_{2n}\text{O}_n$  clusters and, in particular, by  $\text{Li}_4\text{O}_2$ . Clusters actually possess a discrete set of electronic levels, that we will refer to as valence and conduction states. When neutral lithium atoms are added, the number of conduction states increases and the lowest energy ones get filled. As a function of the number, p, of excess lithiums in  $\text{Li}_{4+p}\text{O}_2$  clusters, the electronic structure displays systematic changes in the position of the valence states, the nature of the conduction states, the charge distribution and the HOMO (highest occupied molecular orbital) energy.

#### 4.1 Valence states

The oxygen-derived valence states form two groups (equivalent to the lower and upper valence bands in oxides) associated, respectively, to the oxygen 2s and 2p orbitals. When the number of additional lithiums increases, a systematic shift of these levels towards lower energies is found, as shown in Fig. 4. The variations are better described as a function of the oxygen coordination number which is equal to 3, 4, 4, 5, 5, 6 and 6 in the series. The shift is of the order of 1 eV per unit change in the oxygen coordination number. It may be assigned to an enhancement of the Madelung potential acting on the oxygens, which is created by the positively charged surrounding lithiums. Interestingly, the value of the shift is equivalent to that created by a point charge of +0.12 electron

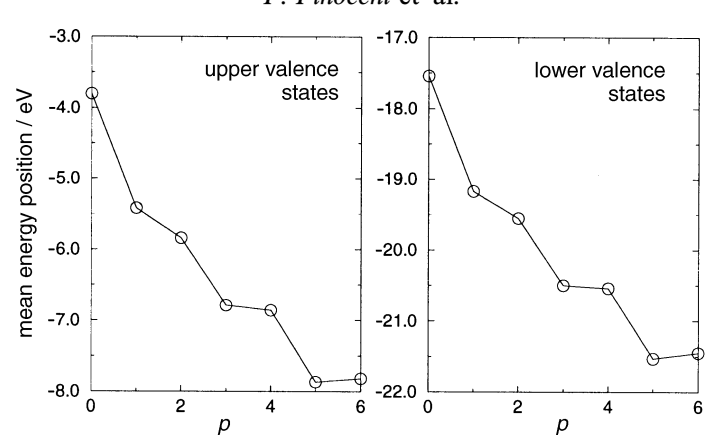


**Fig. 4** Mean energy position of the upper (left panel) and lower (right panel) valence states, as a function of p, for the symmetric  $\operatorname{Li}_{4+p}O_2$  clusters (family II when p is even and family III when p is odd)

located at a distance of 1.7 Å (the average Li—O distance) from the oxygen. This very small value suggests that the lithium atoms in non-stoichiometric clusters cannot be simply interpreted as Li<sup>+</sup> entities. It also suggests that the additional lithium does not remain in a neutral state, otherwise there would be no change in the Madelung potential. A careful analysis of the charge distribution for the higher occupied states is therefore necessary to understand the non-trivial modification of the electronic structure induced by Li adsorption.

#### 4.2 Conduction states

In non-stoichiometric clusters, above the valence states, some conduction states get filled. Plate 1 (a)–(d) represent electron density maps of these states in the two  $\mathrm{Li_6O_2}$  isomers. Several features concerning (i) the delocalization of the wavefunction, (ii) the relative weight of  $\mathrm{Li^{(1)}}$  and  $\mathrm{Li^{(2)}}$  orbitals, (iii) the electron redistribution and (iv) the energy of filled conduction states are worth noting.

- (i) The conduction states are highly delocalized over the whole cluster. By comparison with the valence states, their maximum density is *ca.* two orders of magnitude smaller. The iso-density maps shown in Plate 1 clearly indicate that the wavefunctions have a complex character in which coexist anti-bonding between the oxygen 2s and 2p orbitals and the lithiums as well as collective hybridization between lithium orbitals.
- (ii) Quite systematically [see e.g. Plate 1(c)], in a given cluster, the lowest conduction states have a larger weight on Li<sup>(1)</sup> than on Li<sup>(2)</sup> atoms. This is consistent with the relative values of the Madelung potentials exerted by their oxygen neighbours. This potential raises the lithium effective atomic levels and is stronger on the Li<sup>(2)</sup> than on the Li<sup>(1)</sup>. For the same reason, when inequivalent Li<sup>(1)</sup> are present in an isomer, those located in the most compact part of the cluster have a larger contribution to the lowest conduction states.
- (iii) Each excess lithium brings one electron which is distributed in the whole cluster. All effective lithium charges are decreased, the effect being stronger on the Li<sup>(1)</sup> atoms. The consequence is a weakening of the Li—O bonds, as noted in the previous section.
- (iv) We have reported in Fig. 5 the dependence of the energies of the filled conduction states of both spin directions, as a function of p, in non-magnetic II-Li<sub>4+p</sub>O<sub>2</sub> clusters. The most noticeable feature is the negative slope of these curves which results both

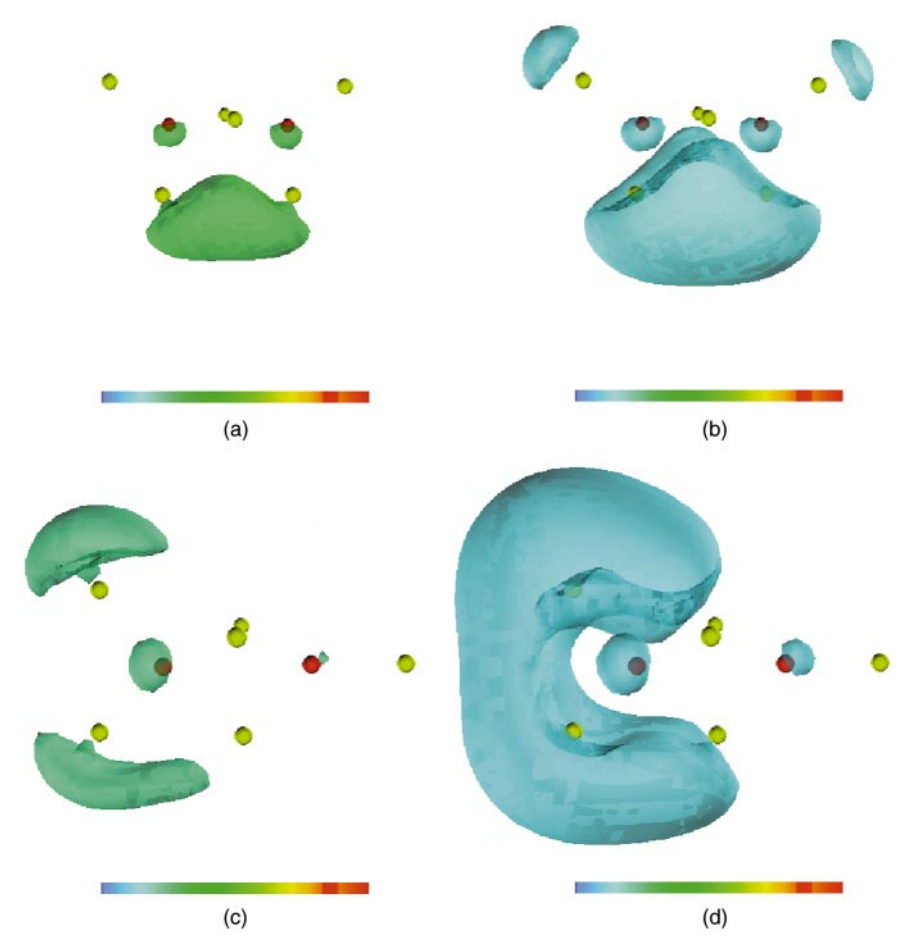


Plate 1 Iso-density surfaces of the HOMO in Li<sub>6</sub>O<sub>2</sub> isomers: (a) and (b) II-Li<sub>6</sub>O<sub>2</sub> at high and low electronic density (25% and 12%, respectively of the maximum density); (c) and (d) III-Li<sub>6</sub>O<sub>2</sub> at high and low electronic density (25% and 12%, respectively, of the maximum density). Atoms are represented by filled spheres, oxygens in red and lithiums in yellow. (a) and (c) evidence the antibonding Li—O character of the conduction states and the relative contributions of inequivalent lithiums; (b) and (d) illustrate the high degree of delocalization of the conduction states.

from a shift of the Li effective levels towards lower energies (same Madelung potential effect as for the valence states) and from an overall increase of the bonding character of the state as it gets delocalized on more lithium atoms. The behaviour is similar for the clusters of the second family. A modification of these curves around p=4 takes place when the magnetic ground state of  $\text{Li}_8\text{O}_2$  is taken into account (see below), but the trend remains unchanged.

The energy difference  $E_i$  between the vacuum level and the cluster HOMO is reported in Fig. 6, as an indication for the variations of the ionization potential of these clusters. The calculation does not take into account self-consistent field relaxation effects, so that only qualitative trends can be discussed.  $E_i$  displays its largest value in the stoichiometric clusters. This is because their HOMO is a valence state, while the HOMO of non-stoichiometric clusters is a conduction state.  $E_i$  also displays odd–even oscillations as a function of p. Whenever a new conduction state starts being filled (for p even), a decrease in  $E_i$  takes place, which is followed by an increase, resulting from the

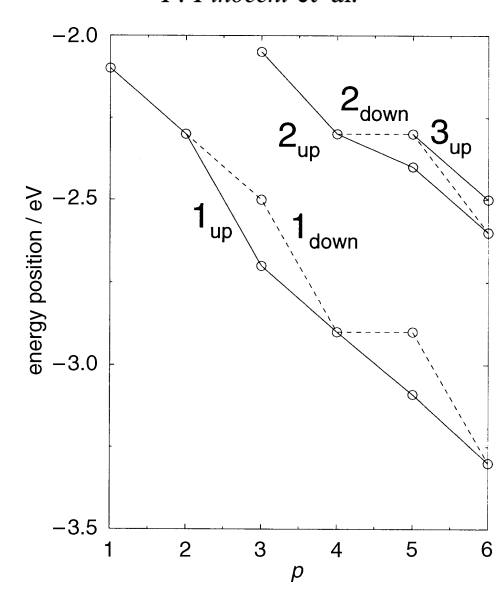
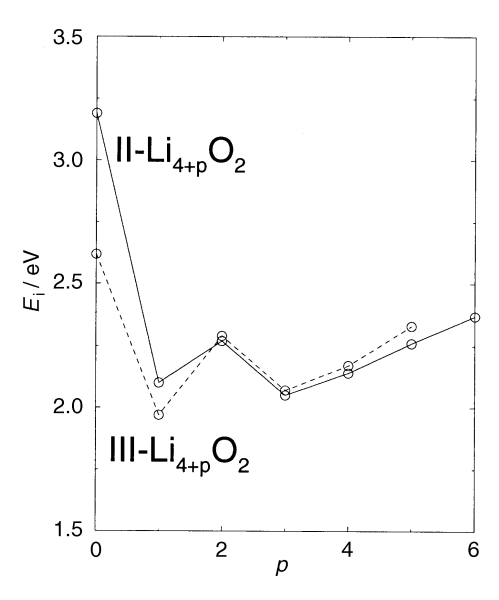


Fig. 5 Energy position of the conduction states, for both spin directions, in non-stoichiometric non-magnetic II-Li<sub>4+p</sub>O<sub>2</sub> clusters, with respect to the vacuum level

negative slope of the level energy curves as a function of p (Fig. 5). The oscillations disappear around p = 4, which is the stoichiometry for which a spin-polarized ground state is found.

In Fig. 7, we have reported the HOMO-LUMO (lowest unoccupied molecular orbital) gap, G as a function of p. Great care should be taken in the interpretation of G, since DFT-LDA theory is, in principle, not designed to yield correct band gaps.<sup>27</sup>



**Fig. 6** Energy difference  $E_i$  between the vacuum level and the HOMO, in non-stoichiometric  $\text{Li}_{4+p}\text{O}_2$  clusters, as a function of p. (——) III- $\text{Li}_{4+p}\text{O}_2$  family; (——) III- $\text{Li}_{4+p}\text{O}_2$  family.

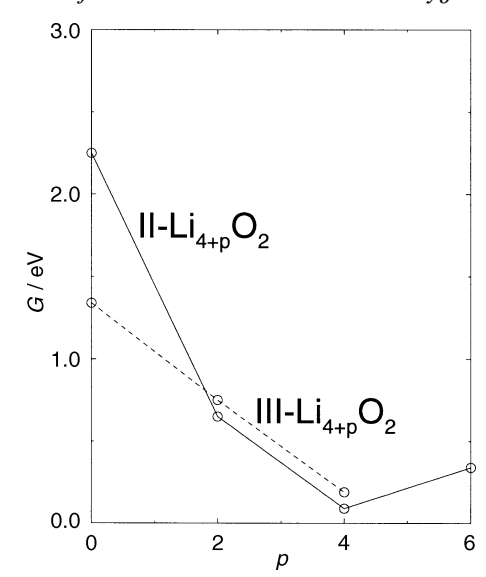


Fig. 7 HOMO-LUMO energy difference, G, in non-stoichiometric  $\text{Li}_{4+p}\text{O}_2$  clusters, as a function of p. Only values for p even are reported. (——) II- $\text{Li}_{4+p}\text{O}_2$  family; (——) III- $\text{Li}_{4+p}\text{O}_2$  family.

However, it gives information on the nature of the conduction states and on the overall stability of the clusters. The stoichiometric clusters display the highest G values owing to the valence character of their HOMO. In Li<sub>4</sub>O<sub>2</sub>, G ranges from 1.3 to 2.3 eV depending upon the isomer, while the LDA gap in bulk Li<sub>2</sub>O is close to 5 eV. More sophisticated ab initio calculations of the self energy in the bulk give 7 eV.<sup>28</sup> Gap variations come partly from differences in the Madelung potentials acting on the atoms in different environments. In the bulk, a large value of the Madelung potential on Li<sup>(4)</sup> and O<sup>(8)</sup> atoms, strongly shifts their effective levels towards higher and lower energies, respectively, thus opening a wide gap. In Li<sub>4</sub>O<sub>2</sub> clusters, the shifts are weaker than in the bulk because of the lower coordination numbers. In non-stoichiometric  $\text{Li}_{4+p}\text{O}_2$  isomers, G decreases as a function of p in the first stages of adsorption. In family II, for example, the low gap values at p = 2 and p = 4 may be understood as resulting from a quasidegeneracy of lithium-derived bonding states, involving, respectively, lithium orbitals from one or the other side of the clusters. This degeneracy is lifted by a structural distortion which brings either one, or two pairs of Li(1), belonging to different ends of the cluster, at a distance characteristic of a Li<sub>2</sub> dimer. It is a Jahn-Teller type distortion. G reaches a minimum value for Li<sub>8</sub>O<sub>2</sub>. Although the HOMO-LUMO gap is not a reliable measure of the actual gap in the excitation spectrum of the clusters, the low G value in Li<sub>8</sub>O<sub>2</sub> suggests the existence of a quasi-degeneracy of the electronic levels close to the Fermi level. It is well known, in Peierls'-type systems for instance, that a small perturbation in the atomic or spin degrees of freedom may in many cases suppress the degeneracy and induce a lowering of the electronic energy. This led us to run LSD calculations for the two Li<sub>8</sub>O<sub>2</sub> isomers to know whether the ground state is spin polarized. In both cases, the answer turned out to be positive with a tiny energy gain of 0.03 and 0.09 eV for the II- and III-Li<sub>8</sub>O<sub>2</sub> isomers, respectively.

# 5 Attachment energy and cluster stability

Understanding the mechanism of the growth of the clusters by attachment of lithium atoms is of key importance, because it can shed some light on the reverse process of

oxygen vacancy formation in oxide materials. Among the two mechanisms of growth, by Li attachment on oxygens or on other lithiums, we will restrict ourselves to the former, and we will show that its probability of occurrence decreases as the number of excess lithiums grows.

We consider two energetic parameters characterizing this growth. The first one is the energy  $\delta_p$  of attachment of a one-fold coordinated  $\mathrm{Li^{(1)}}$  on a  $\mathrm{Li_{4+}}_p\mathrm{O}_2$  cluster, equal to minus the change in energy in the processes:

$$\delta_p(II)$$
: II-Li<sub>4+p</sub>O<sub>2</sub> + Li  $\rightarrow$  II-Li<sub>4+p+1</sub>O<sub>2</sub> (5.1)

$$\delta_p(\text{III}): \text{III-Li}_{4+p}O_2 + \text{Li} \rightarrow \text{III-Li}_{4+p+1}O_2$$
 (5.2)

where we have distinguished the growth of clusters belonging to the II- or the III-family. The second parameter is the attachment energy  $\delta'_p$  of a two-fold coordinated  $\mathrm{Li^{(2)}}$  on a II-Li<sub>4+p</sub>O<sub>2</sub> isomer. It is equal to minus the change in energy in the transformation:

$$II-Li_{4+p}O_2 + Li \rightarrow III-Li_{4+p+1}O_2$$
 (5.3)

Defined in this way, positive values of  $\delta_p$  and  $\delta_p'$  mean that the process of adsorption of the lithium is energetically favoured. Table 1 gives the calculated values of  $\delta_p(II)$ ,  $\delta_p(III)$  and  $\delta_p'$  as a function of p.

Note, in Table 1, that  $\delta'_p$  and  $\delta_p$  are of the same order of magnitude. This could have been expected because of the small energy difference between the parent clusters. Moreover, the attachment energy is only weakly dependent on the site of adsorption (one-fold or two-fold coordination). The values of these energetic parameters compare well with the heat of evaporation of an extra metal atom from  $\operatorname{Li}_p^+(\operatorname{Li}_2\operatorname{O})_n$  with p>1, determined experimentally 10 to be equal to 1.3 eV.

The overall decrease in both  $\delta_p$  and  $\delta'_p$ , as a function of p, shows that the Li enrichment of the cluster through the formation of new Li—O bonds becomes less and less favoured as the cluster size increases. This process is intimately related to the weakening of Li—O bonds, as discussed in Section 4.2, and to the strengthening of Li—Li repulsion. This latter is also responsible for the attachment energies being larger on III-Li<sub>4+p</sub>O<sub>2</sub> than on II-Li<sub>4+p</sub>O<sub>2</sub> clusters, at equal coordination of the oxygens, which arises from the smaller number of Li<sup>(1)</sup> in the former.

The relative stability of the II- and III-Li<sub>4+p</sub>O<sub>2</sub> isomers for a given value of p is illustrated in Fig. 8. The II- and III-isomers are alternatively lower in energy, respectively, for even and odd values of p, up to p=3, and the energy difference decreases as p grows. Beyond p=3 the III-isomers are slightly more stable. However, the disappearance of the oscillation at p=4 is not intrinsic to the geometry or to the charge

**Table 1** Attachment energy,  $\delta_p$ , of Li<sup>(1)</sup> on a cluster Li<sub>4+p</sub>O<sub>2</sub> (in eV) and attachment energy  $\delta_p'$  of Li<sup>(2)</sup> on a II-Li<sub>4+p</sub>O<sub>2</sub> isomer to give a III-Li<sub>4+p+1</sub>O<sub>2</sub> cluster (see text)

p	$\delta_p({\rm II})$	$\delta_p({\rm III})$	$\delta_p'$
0	2.19	2.69	2.56
1	2.27	1.83	2.20
2	1.32	1.43	1.36
3	1.30	1.32	1.36
4	1.26	1.23	1.29
5	1.32		

The numbers in bold represent the largest attachment energy for a given value of p.

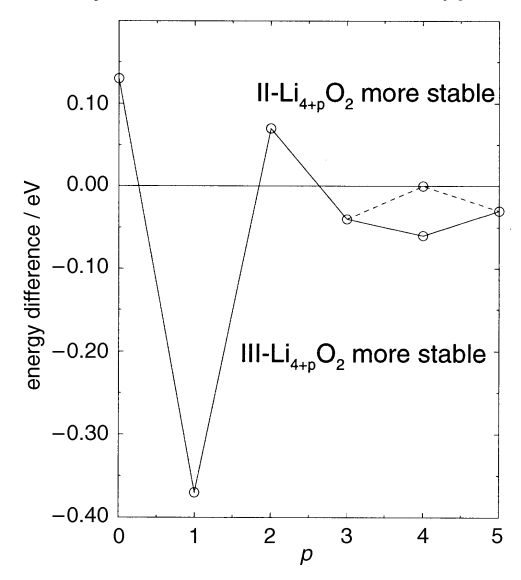


Fig. 8 Energy difference between the III- and II-Li<sub>4+p</sub>O<sub>2</sub> isomers as a function of p, taking into account (——), or not (——), the magnetic ground state of the Li<sub>8</sub>O<sub>2</sub> isomers

distribution. It results from the spin-polarized nature of the ground state of  $\text{Li}_8\text{O}_2$  (see on Fig. 8 the dashed line which refers to the energies in the non-magnetic state). The oscillating behaviour cannot be explained on the basis of changes in the oxygen local environments. Rather, it is a non-local effect, for which the whole cluster shape is important. We propose that the existence of a symmetric environment for the two oxygens (for even values of p in II-isomers, and odd values for III-isomers, see Fig. 2) allows a larger delocalization of the conduction states in the cluster, and thus an increased Li—Li hybridization, which results in a larger stability of the cluster. From the analysis of the dynamical behaviour of the clusters, one can expect, furthermore, that, at non-zero temperatures, entropic effects will enhance the stability of isomers belonging to the II-family.

We thus conclude that the attachment of lithium atoms on oxygens is energetically favoured in the first stages of lithium adsorption. In order to have a qualitative estimate of its competition with the attachment on other lithiums, two energies may be considered: the cohesive energy  $E_{\rm coh}({\rm Li_2})=1.03~{\rm eV^{21}}$  of the Li<sub>2</sub> dimer and the cohesive energy  $E_{\rm coh}({\rm Li})=1.63~{\rm eV}$  per lithium atom in metallic bulk lithium.<sup>29</sup> In pure Li systems, the attachment energy thus increases when the number of Li—Li bonds increases, starting from 1 eV when a single bond is formed, up to 1.6 eV in a bcc environment. Although the charge state of lithiums in the non-stoichiometric clusters is not similar to that in pure lithium systems, we can, nevertheless, anticipate that a change of growth mechanism is likely to occur when  $\delta_p$  becomes smaller than a critical energy bracketed between 1 and 1.6 eV. We will show in a forthcoming publication that, indeed, this transition takes place for p>3.

#### 6 Discussion

Here, we consider the similarities of  $\operatorname{Li}_{4+p}O_2$  clusters to other non-stoichiometric systems, and stress their peculiar features. We successively discuss the degree of delocalization of the filled conduction states, the origin of odd–even oscillations found in differ-

ent physical quantities, the weakening of Li—O bonds and, finally, we consider the numerical approaches potentially designed for such systems.

#### 6.1 Character of the conduction states

The degree of delocalization of the conduction states has been discussed in the context of other non-stoichiometric clusters. In alkali-metal halide  $Na_nCl_{n-x}$  or  $Na_nF_{n-x}$  clusters, for example, it is recognized<sup>30-34</sup> that the excess-electron wavefunction is highly localized and forms an F centre when x=1. The degree of delocalization increases as x grows. At low density of oxygen vacancies, a similar conclusion can be drawn for the bulk and the surfaces of some oxides.<sup>35,36</sup>

By analogy with theoretical arguments proposed to explain the lowering of metal surface work functions upon oxidation,<sup>37</sup> the degree of localization of the HOMO has implications for the value of the ionization potential  $E_{\rm i}$ . Low values of  $E_{\rm i}$  are found whenever the HOMO is strongly localized, owing to a high kinetic contribution to the energy. Conversely, a large delocalization of the electrons in the HOMO is generally related to a large ionization potential.

We find that the conduction states in  $\operatorname{Li}_{4+p}O_2$  are highly delocalized and possess antibonding Li—O character. The electrons do not completely avoid the oxygen region, even though the latter represents a weak contribution to the total wavefunction. In addition, owing to the shape of the central part of the clusters, the charge density associated with the excess electrons does not have a spherical extension, especially at low values of p. The image of excess electrons avoiding the oxygens and moving in a spherical effective potential is thus not supported by our calculations on  $\operatorname{Li}_n O_2$  clusters.

We have found no sign of F centre formation in the first stage of lithium attachment, neither in the II- nor in the III-family. We believe that this result is specific to oxide clusters, in which the creation of an oxygen vacancy in a stoichiometric species requires large topological changes. This conclusion is easily sustained by the examination of the lowest energy  $\mathrm{Li_6O_3}$  and  $\mathrm{Li_8O_4}$  isomers found in our previous study. In Fig. 9, we have reported the structure of  $C_{2v}$ - $\mathrm{Li_6O_3}$ , which yields III- $\mathrm{Li_6O_2}$  upon oxygen removal. In this example, little overall change in the bond topology takes place. However, some lithiums experience large displacements and no sign of the vacancy location remains, neither in the geometry nor in the electronic structure of III- $\mathrm{Li_6O_2}$ . This is at variance with bulk or surface oxides or alkali-metal halide cuboid clusters.



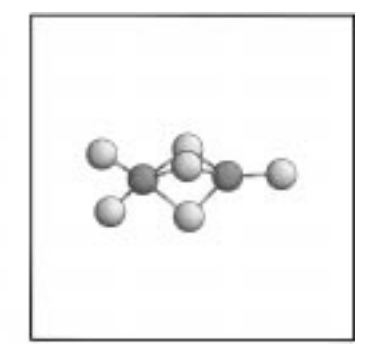


Fig. 9 Stoichiometric  $C_{2v}$ -Li<sub>6</sub>O<sub>3</sub> parent (left) and the non-stoichiometric III-Li<sub>6</sub>O<sub>2</sub> isomer (right). Li atoms are drawn in light grey, O atoms in dark grey, in all ball and stick representations. III-Li<sub>6</sub>O<sub>2</sub> may be obtained by removal of the oxygen located at the bottom of  $C_{2v}$ -Li<sub>6</sub>O<sub>3</sub> and displacements of the neighbouring lithiums.

As far as ionization potentials are concerned, the energy differences between the vacuum level and the HOMO that we have found in non-stoichiometric clusters are lower than those in the stoichiometric clusters and also lower than those obtained by a similar calculation in pure Li<sub>6</sub> and Li<sub>8</sub> clusters (which are *ca.* 3 eV). This is in agreement with the arguments of ref. 37 although, in clusters, the space available for electron delocalization is not a well defined concept.

#### 6.2 Odd-even oscillations

Metallic clusters present odd-even oscillations in the values of the ionization potentials and in abundance patterns obtained in mass spectra, as a result of electron pairing.<sup>38</sup> In non-stoichiometric compound clusters, observation of similar oscillations is considered to be a signature of the presence of a metallic component in the cluster, whether segregation takes place or not.<sup>7,11</sup>

We have found odd-even staggering in the variations of  $E_i$  with p in the two cluster families, for p < 4. Both the presence of oscillations for p < 4 and their absence for p > 4 fit well with the general scheme proposed in ref. 38. This is supported by the similarity between Fig. 6 of the present paper and Fig. 1 of ref. 38, which stresses the role of the spin degeneracy. It is, furthermore, reinforced by the fact that oscillations disappear around p = 4, a stoichiometry at which the spin degeneracy is lifted and the ground state of the clusters becomes magnetic.

The energetic quantity most directly comparable to abundance spectra is the second difference  $\Delta_p = E_{p+1} + E_{p-1} - 2E_p$  expressed as a function of the energies of the clusters containing, respectively, p+1, p-1 and p excess lithiums. We have reported in Fig. 10, the values of  $\Delta_p$  in the two families. There is no well defined signature of oddeven staggering, either in the II- or III-family. The existence of delocalized conduction states is thus not sufficient to induce odd-even oscillations in  $\Delta_p$ . We believe that our result is due to the absence of a segregated lithium part in the clusters and that it

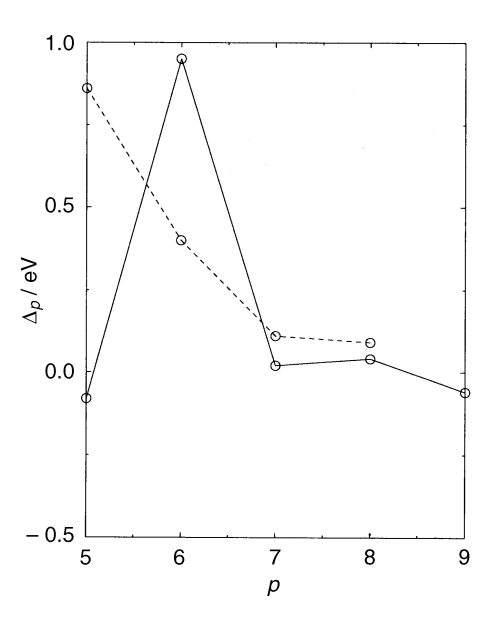


Fig. 10 Second difference  $\Delta_p = E_{p+1} + E_{p-1} - 2E_p$  (in eV) for the two cluster families, as a function of p.  $E_p$  refers to the total energy of an  $\text{Li}_{4+p}\text{O}_2$  isomer. (——) II- $\text{Li}_{4+p}\text{O}_2$  family; (——) III- $\text{Li}_{4+p}\text{O}_2$  family.

stresses the importance of geometrical effects in the physics of non-stoichiometric clusters, as opposed to purely electronic effects.

#### 6.3 Bond weakening

Understanding the mechanism of bond weakening in non-stoichiometric systems gives information on the process of fragmentation, as well as on the interaction strength between vacancies. The calculated values (Section 5) of the energy  $\delta_p$ , required to detach a lithium, suggest that the evaporation of lithium is easier when the overall degree of non-stoichiometry of the cluster is high. It can be related to the weakening of the Li—O bonds, as evidenced by their stretching. Moreover, if one looks at the strength of a particular Li—O bond, Li detachment turns out to be easier from the oxygen with the largest coordination number. This is exemplified by considering the II-Li<sub>5</sub>O<sub>2</sub> isomer, which can yield the II-Li<sub>4</sub>O<sub>2</sub> with  $D_{2h}$  symmetry if an Li<sup>(1)</sup>—O<sup>(4)</sup> bond is broken or the II-Li<sub>4</sub>O<sub>2</sub> with the  $C_{2v}$  symmetry (see Fig. 1) if an Li<sup>(1)</sup>—O<sup>(3)</sup> bond is broken. In the first case, 2.32 eV are required, while in the second case, the detachment costs 3.74 eV. The difference is related to the weaker character of the Li<sup>(1)</sup>—O<sup>(4)</sup> bond, on which the excess electron is more localized.

This result may be compared to the process of vacancy formation in oxides like MgO. There are suggestions from electron-spin resonance, optical absorption or high-resolution electron energy loss spectroscopic experiments, <sup>39-41</sup> as well as theoretical predictions <sup>39,42</sup> that vacancies may cluster. This means that the formation of a second vacancy is easier close to the site where a first one has already been created, as a result of the weakening of neighbouring Mg—O bonds.

#### 6.4 Description of the non-stoichiometry

In the field of insulating materials, pair potential approaches have proven to be a very useful and flexible tool to describe the cohesive properties, morphologies, growth processes, defect diffusion, surface relaxation, segregation etc. They rely on an ionic picture of the materials, in which the two driving types of interactions are the Coulomb charge—charge interactions between ions and the short-range repulsive interactions. To refine the description, van der Waals terms are sometimes added as well as terms accounting for the ion polarisation, usually in the so-called shell model.<sup>43</sup> Parameters are required to make the method operative, for example the ionic charges. They are either fitted to reproduce some given measurable quantities (e.g. the cohesive energy, the bulk phonon dispersion spectrum etc.) or they are derived from ab initio calculations. In both cases, the simplicity of the approach relies on the concept of transferability of the parameters in a variety of systems characterized by different short- and long-range order. Since these methods have been so widely used for describing different physical effects in the field of ionic materials, it is useful to have a perception of how they apply in the case of non-stoichiometric oxide systems.

In our previous study of stoichiometric  $\operatorname{Li}_{2n}O_n$  clusters, we had found that the simple pair potential given in eqn. (3.1) was very helpful in exploring the configurational space and making a selection of low-energy isomers, whose atomic and electronic structures were subsequently refined by means of local *ab initio* minimizations. In many cases, we found that the energy ordering of the isomers was correctly given by the empirical approach, although the energy differences were unreliable. We have searched the maximum degree of non-stoichiometry for which the same potential (with fixed parameters) gives qualitatively good information. Surprisingly, we have found that it correctly predicts the  $\operatorname{III-Li}_5O_2$  isomers to be the most stable, 0.5 eV below the  $\operatorname{II-isomer}$  (0.4 eV in the *ab initio* approach). However, at the next stage of lithium addition, most configurations generated during the annealing cycles led to the detachment of a lithium; a single low-energy isomer of the  $\operatorname{II-type}$  was found. We also tried to simulate

 $\text{Li}_8\text{O}_2$  species but none were stable. The reason for this failure is very obvious. Keeping the ionic charges constant induces a progressive charging of the clusters. The attachment energy of the lithiums decreases drastically as p grows:  $\delta_1 = 2.1$  eV;  $\delta_2 = 0.5$  eV; for  $p \geq 3$ , a too-large repulsion between positively charged lithiums takes place, preventing further growth. This is a physical situation in which the charge distribution is far from that present in the model system on which the fit was performed (bulk  $\text{Li}_2\text{O}$  and the triatomic molecule). Very likely, a pair potential could be built to describe non-stoichiometric clusters, but the parameters should be changed for each lithium content. The method would lose its attraction which comes from the transferability of parameters.

# 7 Conclusions

Ground-state properties of non-stoichiometric lithium oxide clusters  $\operatorname{Li}_{4+p}O_2$   $(p \le 6)$  have been studied by means of AIMD simulations. The present study is restricted to the investigation of the low-energy isomers in which all lithiums are bound to oxygens. The structure, bonding properties and stability have been analysed as a function of the number, p, of excess lithiums.

We have found two families of isomers for each lithium content, in which the two oxygens are bridged by either two or three lithiums. Their energies are very close to each other, the most stable isomer being the one in which the two oxygens have the same coordination number. Formation of six Li-O bonds around each oxygen marks the final step of stable lithium attachment that we find. The largest size clusters are two Li<sub>6</sub>O octahedra sharing an edge (II-Li<sub>10</sub>O<sub>2</sub>) or a face (III-Li<sub>9</sub>O<sub>2</sub>), the latter configuration being isostructural with the Rb<sub>9</sub>O<sub>2</sub> entity, found to be the building block of Rb<sub>9</sub>O<sub>2</sub> and Rb<sub>6</sub>O suboxides.<sup>25</sup>

The electronic structure of  $\operatorname{Li}_{4+p}O_2$  clusters is characterized by the progressive filling of conduction states, of Li-O antibonding character, that we have found to be highly delocalized. The relative contributions of inequivalent lithium orbitals to the conduction states may be related to the Madelung potentials acting on these atoms, which raise up to a different degree their effective atomic levels. An Li-O bond expansion is induced by the filling of conduction states, which is revealed by the progressive decrease of the Li attachment probability as p grows. The presence of even-odd staggering in electronic-related quantities (the vacuum-HOMO energy difference) and their absence in energetics quantities (the second difference in total energies) reveals the subtle interplay between electronic and geometric effects in these families of non-stoichiometric clusters.

Relying upon the relative values of the attachment energies that we find, and those expected in pure lithium systems, we argue that a cross-over takes place at intermediate values of p (p > 3) towards another growth mechanism by attachment of lithiums on other lithiums. The thorough investigation of this mechanism is the subject of a forth-coming paper.

Calculations were performed on the Cray C98 at the IDRIS computational centre in Orsay (project 960109). We thank the IDRIS staff for helpful collaboration and technical assistance and in particular T. Goldmann for his help in the use of the AVS application (Plate 1). Fig. 1, 2 and 9 were drawn using the RasMol program developed by Roger Sayle. Useful discussions with C. Bréchignac and M. De Frutos are gratefully acknowledged.

#### References

1 V. E. Henrich and P. A. Cox, The Surface Science of Metal Oxides, Cambridge University Press, Cambridge, 1994.

- 2 C. Noguera, Physics and Chemistry at Oxide Surfaces, Cambridge University Press, Cambridge, 1996; Physique et Chimie des Surfaces d'Oxydes, Eyrolles, 1995, collection Alea.
- W. A. Saunders, Phys. Rev. B, 1989, 37, 6583.
- 4 T. P. Martin and T. Bergmann, J. Chem. Phys., 1989, 90, 6664
- 5 P. J. Ziemann and A. W. Castleman, J. Chem. Phys., 1991, 94, 718.
- 6 A. Nakajima, T. Sugioka, K. Hoshino and K. Kaya, Chem. Phys. Lett., 1992, 189, 455.
- 7 T. Bergmann, H. G. Limberg and T. P. Martin, Phys. Rev. Lett., 1988, 60, 1767.
- 8 H. G. Limberg and T. P. Martin, J. Chem. Phys., 1989, 90, 2979.
- 9 T. Bergmann and T. P. Martin, J. Chem. Phys., 1989, 90, 2848.
- 10 C. Bréchignac, P. Cahuzac, F. Carlier, M. de Frutos, J. Leygnier and P. Roux, J. Chem. Phys., 1993, 99,
- 11 C. Bréchignac, Ph. Cahuzac and M. de Frutos, personal communication.
- 12 T. P. Martin and B. Wassermann, J. Chem. Phys., 1989, 90, 5108.
- 13 P. Wang and W. C. Ermler, J. Chem. Phys., 1991, 94, 7231.
- 14 J. M. Recio and R. Pandey, Phys. Rev. A, 1993, 47, 2075.
- 15 M. J. Malliavin and C. Coudray, J. Chem. Phys., 1997, 106, 2323.
- 16 S. Moukouri and C. Noguera, Z. Phys. D, 1993, 27, 79.
- 17 F. Finocchi and C. Noguera, Phys. Rev. B, 1996, 53, 4989
- 18 R. Car and M. Parrinello, Phys. Rev. Lett., 1985, 55, 2471.
- 19 L. Kleinman and D. M. Bylander, Phys. Rev. Lett., 1982, 48, 1425.
- 20 N. Troullier and J. L. Martins, Phys. Rev. B, 1991, 43, 1993.
- 21 J. Vergès, R. Bacis, B. Barackat, P. Carrot, S. Churassy and P. Crozet, Chem. Phys. Lett. 1983, 98, 203.
- 22 I. Boustani, W. Pewerstorf, P. Fantucci, V. Bonacic-Koutecky and J. Koutecky, Phys. Rev. B, 1987, 35, 9437.
- 23 V. Bonacic-Koutecky, I. Boustani and J. Koutecky, Int. J. Quantum Chem., 1990, 38, 149; and personal communication
- 24 T. P. Martin, Physica B, 1984, 127, 214.
- 25 A. Simon, in Crystal Structure and Chemical Bonding in Inorganic Chemistry, ed. C. J. M. Rooymans and A. Rabenau, North Holland Publishing, Amsterdam, 1975.
- 26 R. D. Shannon, Acta Crystallogr. Sect. A, 1976, 32, 751.
- 27 R. W. Godby, M. Schlüter and L. J. Sham, Phys. Rev. Lett., 1986, 56, 2415; Phys. Rev. B, 1988, 37, 10159.
- 28 S. Albrecht, G. Onida and L. Reining, Phys. Rev. B, 1997, 55, 10278.
- 29 C. Kittel, Introduction to Solid State Physics, Wiley, New York, 1976.
- 30 U. Landman, D. Scharf and J. Jortner, Phys. Rev. Lett., 1985, 54, 1860.
- 31 E. C. Honea, M. L. Homer, P. Labastie and R. L. Whetten, Phys. Rev. Lett., 1989, 63, 394.
- 32 G. Rajagopal, R. N. Barnett and U. Landman, Phys. Rev. Lett., 1991, 67, 727.
- 33 P. Xia and L. A. Bloomfield, Phys. Rev. Lett., 1993, 70, 1779.
- 34 R. N. Barnett, H. P. Cheng, H. Hakkinen and U. Landman, J. Phys. Chem., 1995, 99, 7731.
- 35 L. N. Kantorovich, J. M. Holender and M. J. Gillan, Surf. Sci., 1995, 343, 221.
- 36 A. M. Ferrari and G. Pacchioni, J. Phys. Chem., 1995, 99, 17010.
- 37 M. G. Burt and V. Heine, J. Phys. C: Solid State Phys., 1978, 11, 961.
- 38 M. Manninen, J. Mansikka-aho, H. Nishioka and Y. Takahashi, Z. Phys. D, 1994, 31, 259.
- 39 K. C. To, A. M. Stoneham and B. Henderson, Phys. Rev., 1969, 186, 1237.
- 40 B. Henderson and D. H. Bowen, J. Phys. C, 1971, 4, 1487.
  41 M. C. Wu, C. M. Truong and D. W. Goodman, Phys. Rev. B, 1992, 46, 12688.
- 42 E. Castanier and C. Noguera, Surf. Sci., 1996, 364, 17.
- 43 W. Cochran, Crit. Rev. Solid State, 1971, 2, 1.

Paper 7/02171B; Received 1st April, 1997